An approach on the comparative behavior of chloro / nitro substituted phenols photocatalytic degradation in water

A. Tolosana-Moranchel[b*], D. Ovejero[a], B. Barco[a], A. Bahamonde[a], E. Díaz[b], M. Faraldos[a*]

[a] Instituto de Catálisis y Petroleoquímica, ICP-CSIC, C/ Marie Curie 2, 28049 Madrid, Spain.

[b] Dep. Ingeniería Química, Fac. de Ciencias, C/ Francisco Tomás y Valiente 7, Universidad Autónoma de Madrid, 28049 Madrid, Spain.

ABSTRACT

The study of position and number of substituents on the photocatalytic removal of some mono-, di- and tri-, chloro- and nitrophenols, as well as more known initial TOC concentration effect, has revealed the noteworthy impact on the process efficiency. Despite the complex effect of multiple substituents directing the HO• attack to their preferential positions, Hammett constant could be used to predict photocatalytic degradation performance. TiO_2 P25 was able to mineralize initial TOC concentrations up to 25-50 $mg \cdot L^{-1}$. Higher TOC concentrations constitute a drawback and drive to residual parent pollutants and organic by-products, which become more important when raising the starting TOC loading. Increasing the number of chloro- or nitro- groups in the aromatic ring does not imply higher ecotoxiticy values; contrarily, the position of the substituent can lead to significant differences. TOC conversion values are hardly affected by the substituent position, but by the number of groups in the organic molecule, probably due to steric hindrance. The formation of chloride and nitrogen inorganic ions, inherent to photocatalytic degradation, fulfills the Cl and N mass balances. Finally, the effect of number, position and electronic nature of substituents on contaminant initial photocatalytic degradation rates was studied by corresponding Hammett constant correlations.

Keywords: Hammett constant, photocatalytic degradation, TiO_2, chlorophenols, nitrophenols

INTRODUCTION

Nowadays, water pollution is one of the biggest issues of environmental protection field in the world [1]. From regulations, projects and awareness campaigns, politicians and scientists are working together to find better ways to manage wastewaters.

Phenolic compounds are persistent organic pollutants commonly present in industry effluents from agriculture, dyestuffs, petroleum, pesticide, paper, pharmaceuticals [2,3,4]. Consequently, they can be found in wastewaters at low concentrations (10 – 100 mg/L) from cleaning containers or spills and also at high concentrations (~ 1000 mg/L) from wastewater generated in oil refinery or olive mill [5,6]. Specifically, substituted phenols (nitro- and chloro-) are characterized by a good water solubility, high toxicity and poor biodegradability and, consequently, most of them are included in the “Priority Pollutants List” by the US Environmental Protection Agency (EPA) [7,8].

One of the most promising goals in the field of wastewater treatments is focused on the development of technologies able to remove these hazardous pollutants and obtain high quality water effluents before discharging into aquatic environment. Advanced Oxidation Processes (AOPs) are considered a potential alternative to deal with recalcitrant organic pollutants. Heterogeneous photocatalysis using TiO_2, based on the hydroxyl radical generation through the e^-/h^+ pairs generated when the semiconductor is exposed to UV radiation, is by far the most studied oxidation process for the mineralization of pollutants into harmless products (carbon dioxide, water and inorganics) [9]. Recently, other photocatalytic hybrid materials, based on metal-doped semiconductors [10,11], transition metal calcogenures [12], g-C_3N_4 [13], graphene derivatives [14,15,16], MOFs [17,18] have

been applied trying to combine different strategies, such as widen UV-Vis radiation harvesting, improve adsorption, increase lifetime of photogenerated charges, etc., to enhance photocatalytic processes efficiency.

The main advantages of photocatalysis over other AOPs lie in the employ of a cheap, active and stable catalyst, no addition of chemicals, the operating conditions (ambient temperature and pressure) and the possibility of using renewable energy sources, which reduce treatment costs. Good results have been obtained by application of photocatalysis on the industrial wastewater with aromatics [19,20], pesticides [21,22,23], pharmaceuticals [24,25,26,27], as also on the application of photocatalysis in water disinfection [9,28,29].

Photocatalytic efficiency of chloro- and nitro-phenols degradation has been demonstrated and studied in terms of initial pH, influence of anions, light intensity, dosage of catalyst, or using photocatalyst other than TiO_2 [30,31,32,33,34,35]. Some previous studies, carried out for some specific chloro- and nitro-phenols, pointed to the influence of both electronic character and position of the substituent groups in the aromatic ring, as well as adsorption contribution to contaminants removal [36,37,38].

In this context, the main objective of this work has consisted on studying the influence of position and number of substituents on the photocatalytic degradation of mono-, di- and tri-chloro- and nitro-phenols in aqueous effluents. For that a comparative study of the effect of TOC loading on ecotoxicity reduction along photocatalytic degradation of these chlorophenols (CPs) and nitrophenols (NPs) contaminants was performed, analyzing the different reactivity and riskiness of implicated compounds. Subsequently, corresponding Hammett constant will be used to achieve the definition of a generic correlation between the number, position and electronic nature of the substituents, and initial photocatalytic degradation rate of each CP and NP. TiO_2 P25 photocatalyst was selected due to the

complete characterization studies previously reported [39,40] and wide knowledge about photocatalytic degradation performance [36,41,42,43].

2. EXPERIMENTAL SECTION

2.1 Materials

Photocatalytic experiments were carried out employing commercial titanium dioxide P25 Aeroxide® from Evonik Degussa.

Analytical grade organic pollutants: 4-chlorophenol (4-CP), 2,4-dichlorophenol (2,4-DCP), 2,5-dichlorophenol (2,5-DCP), 2,4,5-trichlorophenol (2,4,5-TCP), 4-nitrophenol (4-NP), 2-nitrophenol (2-NP) and 2,4- dinitrophenol (2,4-DNP) were purchased from Sigma-Aldrich (now Merck) and used without further purification. Solutions of CPs and NPs were prepared in Milli-Q water at natural pH. All reagents used for chromatographic analyses: (Milli-Q water, methanol, 2,6-pyridinedicarboxylic acid, ortho-phosphoric acid, sulfuric acid, nitric acid, and sodium carbonate) were HPLC grade.

2.2 Photocatalytic activity

Photocatalytic degradation runs were carried out in a stirred 1L cylindrical Pyrex semi-continuous slurry photoreactor set in a Multirays apparatus (Helios Italquartz), previously described in detail [44]. The system was made up of highly reflective aluminum sheets enclosing the Multirays apparatus' interior walls, to make the most of the scattered radiation, and ten lamps located around the cylindrical photoreactor, which provided a total irradiance value of 38 $W \cdot m^{-2}$ in the UV-A range (306-383 nm). Two different types of 15 W lamps (6 Narva BlackLight Blue and 4 Narva 865 cool daylight) were used.

Photocatalytic reactions were carried out under constant stirring at atmospheric pressure, room temperature and bubbling a continuous air flow (75 $Ncm^3 \cdot min^{-1}$). 1 L of solution of the corresponding organic pollutant concentration was poured into the photoreactor and then a previously optimized catalyst-loading equivalent to 200 $mg \cdot L^{-1}$ of P25 was added too. The suspension was mixed for 30 minutes to ensure the adsorption step was completed and mixture homogeneity achieved. Afterwards, all the lamps were turned on to start photodegradation experiments. Samples were taken out at given reaction times and filtered by using PTFE syringe filters (25 mm diameter, 45 μm sieving size). The study was performed in a wide range of concentrations, from 12.5 to 400 $mg_{TOC} \cdot L^{-1}$.

Chloro- and nitrophenols and their aromatic intermediates were identified and quantified by means of High Performance Liquid Chromatography HPLC (Varian 920 LC) with photo-diode array detector. A Nucleosil C18 5 μm column (15 cm long, 4.6 mm diameter) was used as stationary phase at 40 ºC. Mobile phase flow was 0.8 mL min^{-1} and 20/80% v/v methanol/acidic water (0.1% phosphoric acid) mixture were used as solvents.

Chlorides, nitrates, nitrites ions and short-chain organic acids were measured by Ion Chromatography with chemical suppression (Metrohm 883 IC) and a conductivity sensor, using a Metrosep A supp 7-250 column (250 mm long, 4 mm diameter) as stationary phase and 3.6 mM sodium carbonate as eluent. When Ammonium ions and other cations were detected the stationary phase was a Metrosep C 6-250 column (250 mm long, 4 mm diameter) and 1.7-1.7 mM nitric acid-dipicolinic acid was the mobile phase.

TOC concentrations of extracted aliquots were detected by an infrared-detector TOC-$V_{CSH/CSN}$ Shimadzu analyzer.

2.3 Ecotoxicity evaluation: Microtox® test

The ecotoxicity test was carried out in the Microtox M500 toxicity analyzer according to the standard procedure [45]. The lyophilized bacteria *Vibrio fischeri* was purchased from Azur Environmental. Toxicity units were calculated measuring the inhibition of the light emission by the bacteria after 15 min contact time with the samples. Moreover, EC_{50} values of each pollutant, which indicate the effective compound concentration causing 50 % reduction of light emission, were also obtained.

3. RESULTS AND DISCUSSION

3.1. Influence of initial concentration

Before photocatalytic degradation tests, blank experiments in the absence of photocatalyst and in dark conditions, were carried out, at the same operating conditions. Non-photocatalytic degradation of contaminants was negligible. Contaminants removal due to adsorption was proportional to the number of Cl- substituents for CPs, being around 4% for 4-CP; 10% for 2,4-DCP and 2,5-DCP; and approximately 15% in the case of 2,4,5-TCP in concordance with previously reported results [32]. However, the NPs removal due to adsorption contribution was considerably lower and hardly achieved 5% of initial concentration, independently of initial concentration or number of $-NO_2$ substituents, congruent with earlier findings [37].

The photocatalytic degradation of different concentrations of 4-CP and 4-NP has been followed versus irradiation time, analyzing the efficiency of the photocatalytic system. Whereas initial loadings of 4-CP lower to 50 $mg_{TOC}\cdot L^{-1}$ concentration were completely photocatalytically degraded after 300 min (**Figure 1A**), longer times were required to photodegrade lower TOC concentrations, such as 25 $mg_{TOC}\cdot L^{-1}$, in the case of 4-NP (**Figure 1C).** Conversion of contaminant, and organic matter in general, even diminishes

dramatically for higher initial TOC content (**Table 1**), what is associated with the formation of intermediates, most of them non-aromatic compounds in the case of the studied phenol derivatives [46,47,48,49].

The photocatalytic degradation pathway for 4-CP goes through the formation of hydroxylated intermediates (4-chlorocathecol and benzoquinone-hydroquinone) that further oxidize to short-chain organic acids (maleic, malonic, oxalic, acetic and formic), following the scheme showed in Figure S1, all of them detected by HPLC and IC, respectively. The generation of chlorinated-aromatic-intermediates seems to be the responsible of the ecotoxicity maximum found at middle irradiation times [50]. In the case of 4-NP, the photo-oxidation route also begins by the rapid hydroxyl radical attack to form the di-hydroxynitrobenzenes, followed by a second step where the aliphatic chains were slowly oxidized [51], before mineralization was reached. Whereas no aromatic intermediates (4-nitrocathecol, nitrohydroquinone-benzoquinone and 1,2,4-trihydroxybenzene) [52,46] of the proposed mineralization pathway (Figure S1), were detected by HPLC, probably due to their short lifetime in the reaction medium; oxalic and formic acid (not shown), and ammonium, nitrite and nitrate ions were detected and quantified (**Figure 1D**). The short-chain organic acids found mainly corresponded to formic acid (0.1-0.4 $mg \cdot L^{-1}$) for 12.5 and 25 $mg \cdot L^{-1}$ initial concentrations of 4-NP, respectively, and some residual oxalic acid (~ 0.2 $mg \cdot L^{-1}$) contribution for 50 $mg \cdot L^{-1}$ of initial 4-NP concentration. In both cases 4-CP and 4-NP photocatalytic degradation provokes an acidification of the reaction media from initial pH ≅ 5-6 to ≅ 3 and ≅ 3.5, respectively, due to the formation of the afore-mentioned short-chain organic acids.

As expected, mineralization of 4-CP leads to an increase of chloride ion concentration **(Figure 1B)**; in fact, the 85-100% of the initial chlorine content in original 4-CP was found as chloride in the reaction medium for initial TOC concentrations up to 100 $mg \cdot L^{-1}$ (**Table**

1) fulfilling Cl mass balance. 4-chlorocathecol was the predominant intermediate in the case of 4-CP concentrations higher than 100 $mg_{TOC}·L^{-1}$, reaching values of 54 $mg·L^{-1}$ and 40 $mg·L^{-1}$, after 300 minutes of irradiation time, for 400 $mg_{TOC}·L^{-1}$ and 200 $mg_{TOC}·L^{-1}$ 4-CP initial concentration, respectively. However, hydroquinone was more relevant for lower initial concentrations of 4-CP, with values among 0.7-10 $mg·L^{-1}$, for 4-CP initial concentration under 200 $mg_{TOC}·L^{-1}$, indicative of a faster photocatalytic degradation.

Contrarily, the photodegradation of 4-NP presented a nitrogen mass balance that always fulfils when the sum of unreacted 4-NP, minor 4-aminophenol (4-AP) and inorganic ammonium (NH_4^+), nitrite (NO_2^-) and nitrate (NO_3^-) was considered; what points to the absence of other relevant aromatic nitrogen intermediates. Then, all 4-NP oxidizes via a first step of denitrification that rapidly evolves to short-chain organic acids before complete mineralization. Consequently the nitrogen present in the system could be found as 4-NP, NH_4^+, NO_2^- and/or NO_3^- (**Table 1**). At the end of irradiation time, the composition of the reaction media varied from majority NO_3^- (6 - 9 $mg·L^{-1}$) with traces of NO_2^- (3 - 0.3 $mg·L^{-1}$) and 4-AP (0.14 - 0.24 $mg·L^{-1}$), in the case of 12.5 and 25 $mg_{TOC}·L^{-1}$ initial concentration, respectively; to a larger number of intermediates in the mixture for higher initial 4-NP concentration (50 $mg_{TOC}·L^{-1}$), where NH_4^+ (maximum 0.3 $mg·L^{-1}$) was detected at middle irradiation times, being oxidized to NO_2^- (3 $mg·L^{-1}$) and NO_3^- (5 $mg·L^{-1}$) after 300 minutes, indicating a lower oxidation step in this photocatalytic degradation reaction.

Trying to analyze and compare the evolution of the organic and inorganic species generated along the photocatalytic degradation reaction of chloro- and nitrophenols, the initial rates of photocatalytic degradation and formation of the different identified species have been calculated for the different compounds and concentrations (**Figure 2**).

The initial rate of NPs photocatalytic degradation follows similar trends regardless of the initial TOC concentration (**Figure 2A-C**) and only for 4-NP a slight decrease could be

observed from 12.5 to 25 mg·L^{-1} that was smoother when the initial concentration was 50 mg·L^{-1} (**Figure 2A**). However, the initial rates of ammonium, nitrite and nitrate ions formation, coming from 4-NP photocatalytic degradation route, showed significant differences. While nitrite and nitrate generation becomes inhibited at higher 4-NP concentrations, ammonium performs the opposite (**Figure 2A**). This fact corresponds to species formed in the first step of the photocatalytic degradation route that suffer further oxidation until nitrite or nitrate. The origin could be the photocatalytic degradation of 4-NP taking place through the 4-aminophenol (4-AP) intermediate [53], which was detected in some cases but at very low concentration, almost in the limit of quantification (LoQ) of the HPLC instrument. Concerning 4-CP photocatalytic degradation, chloride formation did not depend on the initial TOC loading (**Figure 2D**), but 4-CP initial photocatalytic degradation rate became speeded up at higher initial 4-CP concentration.

3.2. Influence of substituents: position and number.

The photocatalytic degradation of phenolic compounds initially proceeds through the diffusion controlled addition of HO•, a strong electrophile, with high affinity for the electron-rich sites of these aromatic compounds. In the case of p-substituted phenols, $HO^{\bullet}$ reacts with the unsubstituted positions more negatively charged. When more substituents are present, the concerted effects (electronic distribution and steric factors) in controlling the reaction site could drive to substitution (*ipso* addition + elimination) or *ortho*, *meta*-addition. In the case of 4-CP, both –OH an –Cl groups are electron-withdrawing and provoke a similar inductive effect in the atoms, but the dominant effect of –OH, reinforced by –Cl, favors the preferential addition of HO• to its relative *ortho* > *para* position, where a greater negatively charged density is located [54]. Meanwhile, the *para* position of another electron-withdrawing substituent, $–NO_2$ group, in 4-NP helps to delocalize the electrons in

the aromatic ring and promote HO• addition in *meta* > ipso position (relative to –OH) where, in this case, more electron density was accumulated [55].

The confluence of multiple substituents on the aromatic ring could have additive effects as observed in the case on 4-CP, but the directed position to HO• addition was the sum of various factors: relative electronic density of each position, steric control, electron-withdrawing character of substituents, and resonance effect. Even when both substituents have similar inductive behavior, the reinforced HO• attach positions could be different, depending on the charge distribution.

In this sense, trying to elucidate the role of substituents position on the preferential HO• attack and the primarily formed by-products, the photocatalytic degradation of 2-nitrophenol (2-NP) compared to 4-NP, and 2,4-dichlorophenol (2,4-DCP) versus 2,5-dichlorophenol (2,5-DCP) was investigated along irradiation time (**Figure 3A-D**). 2-NP achieved hardly 5% more conversion than 4-NP **(Figure 3 C-D)** (69% and 66% of 2-NP and 4-NP conversion at 25 $mg_{TOC} \cdot L^{-1}$ initial concentration, respectively), similar mineralization degree and slightly higher TOC initial rate **(Table 2)**. Electron-donor substituents, such as –OH, increase electronic density on *ortho*- and *para*- positions favoring the HO• attack [50,54], while $–NO_2$ promotes *meta*-directing HO• addition. In this situation 2-NP has available both position to initiate the photocatalytic degradation pathway, although the *para*-addition is reinforced by both substituents, where the main intermediate should be hydroquinones. Meanwhile, in 4-NP, both –OH and $–NO_2$ substituent strengthens *ortho*-attack [47]. In this situation, where initial steps could go through different intermediates, NPs and TOC initial photocatalytic degradation rates and conversions did not present a parallel behavior. Then, mineralization degree reached lower values than pollutant conversion at the different initial 2-NP concentrations (e.g. 29 - 69 - 100 % of 2-NP, and 25 - 61 - 88 % of TOC conversion, were achieved for 12.5 - 25 -

50 $mg_{TOC}·L^{-1}$ initial concentration, respectively), with residual concentrations of short-chain organic acids, mainly formic (0 - 1.5 $mg·L^{-1}$) and oxalic (0 - 0.8 $mg·L^{-1}$) acids remaining in the reaction media together with nitrite (0 - 2.3 $mg·L^{-1}$), nitrate (5 - 8.3 $mg·L^{-1}$) and minimal amounts of ammonium (< 0.5 $mg·L^{-1}$) ions, at final irradiation times. 4-NP presented a similar performance (e.g. 41 - 66 - 100 % of 4-NP, and 27 - 57 - 95 % of TOC conversion, for 12.5 - 25 - 50 $mg_{TOC}·L^{-1}$ initial concentration, respectively), with residual formic (0.1 - 1.0 $mg·L^{-1}$) and oxalic (0 - 0.6 $mg·L^{-1}$) acids, nitrite (0.3 - 3 $mg·L^{-1}$) and nitrate (9.1 – 6.0 $mg·L^{-1}$) ions, remaining in the reaction media at final irradiation times.

2,5-DCP and 2,4-DCP were completely removed after 360 minutes of irradiation time, but the photocatalytic degradation progresses through different pathway. During 2,5-DCP photocatalytic degradation, hydroquinones and 4-chlorocathecol could be identified, revealing the directing action of –OH to *ortho* and *para* attack reinforced by –Cl in position 5. Meanwhile, in the case of 2,4-DCP only hydroquinone could be detected due to the absence of empowered positions that results in the –OH direction towards *para* addition [56].

The study was completed with 2,4,5 trichlorophenol (2,4,5-TCP) and 2,4-dinitrophenol (2,4-DNP) looking for the role that the number of substituents could play throughout photocatalytic degradation and further mineralization of original compounds. Taking into account that halogen and nitro groups are highly electronegative, the increase of the number of these electron-withdrawing substituents reduces the electronic density of the aromatic ring that could provoke a lower affinity to photocatalytic oxidation [57]. This effect will be compensated in the case of halogens because they have lone pairs of electrons to be shared with the aromatic ring, explaining the more reactive character showed by 4-CP in contrast to 4-NP at the same initial concentration of 25 $mg_{TOC}·L^{-1}$. In both cases the photocatalytic degradation implies the addition of HO• in reinforced positions, mainly *ortho*

and *para* respecting to –OH [58,59], with steric hindrance conditioning the selectivity and kinetics of the reaction [56]. Therefore, the higher number of substituents the more difficult access of HO• that causes the CPs and NPs initial photocatalytic degradation rate to slow down, as can be observed in **Figures 2 E** and **A-C**, respectively.

Considering the profile of 4-NP photocatalytic degradation versus 2-NP and evolution of 2,4-DCP concentration versus 2,5-DCP **(Figure 3C** and **3A**, respectively) during irradiation time, initial photocatalytic degradation rates **(Figure 2A, B** and **E**) were not significantly altered by the position of substituents. Similar results were observed for TOC initial photocatalytic degradation rate in the case of CPs (**Table 2**) [60]. However, higher concentration of chlorine in the parent pollutant for the same TOC content favored the generation of chloride in the reaction media (**Figure 3B**). On the other hand, the initial rate of chloride formation increased with the number of chlorine substituents (**Figure 2E**), observing no effect of their position on the aromatic ring in the kinetic parameters. The presence of nitrogen ions in the reaction media at final irradiation time was proportionally growing with the nitrogen content in the parent contaminant (**Figure 3D**), but the differences were not as remarkable as in the case of CPs, mainly due to its moderate reactivity that conduces to lesser conversion and inorganic ions concentration in solution, as corresponds to lower mineralization degree. Equally, the variation of initial rate of inorganic nitrogen ions formation appears affected by the higher number of nitro-substituents that led to faster nitrate generation at the first steps of 2,4-DNP photocatalytic degradation, while ammonium and nitrite barely change (**Figure 2A-C**).

Respecting to ecotoxicity, initial toxicity of NPs was significantly lower than corresponding studied CPs (**Table 3**). The ecotoxicity for the studied chorophenols follows the sequence expressed as EC_{50}: 2,4,5-TCP ≈ 4-CP > 2,4-DCP >> 2,5-DCP. In the case of nitrophenols, 2-NP and 2,4-DNP present similar EC_{50} values while 4-NP was significantly more toxic.

According to these values, it is essential that photocatalytic degradation treatment causes a high removal rate of the chlorinated compounds to achieve a significant toxicity reduction. Moreover, a high mineralization degree is also desired in the case of reaction intermediates can provide more toxicity than starting pollutants to reaction medium [49]. Regarding to TU values obtained for reaction effluents, the photocatalytic treatments promoted a dramatically decrease of the ecotoxicity in all the cases, transforming the pollutants into innocuous products (Table 3).

3.3. Hammett constant: Effect of the electronic character of substituents on CPs and NPs degradation.

Since the pollutants investigated in this study were substituted phenols, it might be interesting to correlate their photocatalytic removal with the electronic nature, number and position of the substituents [61]. As a result, a prediction of their photocatalytic degradability could be made based on their electronic character. Previous studies correlated the Hammett constant (σ) to the disappearance of aromatic compounds [37,61,62] where it was found that photocatalytic degradation was faster in the case of groups that involved a greater electron density.

The Hammett constant (σ) values are numbers that sum up the total electrical effects (resonance plus field effects) of a group when attached to a certain aromatic system, phenol in this study. A positive value of σ indicates an electron-withdrawing group and a negative value an electron-donating group. When the initial photocatalytic degradation rates ($-r_0$) for the different used compounds were plotted, in **Figure 4**, against the Hammett constant values (σ) [37,63,64], a correlation could be established for each series of compounds, CPs and NPs, with R^2=0.969 and R^2=0.976 respectively, supporting the

influence of electronic character of Cl− and $-NO_2$ substituents on the CPs and NPs photocatalytic degradation.

Regarding CPs, the higher the number of -Cl groups, the slower the degradation rate as this implied a lower electron density in the aromatic ring. Some authors found no influence of the substituent position in the photocatalytic degradation except for dihydroxybenzenes [61]. However, **Figure 4** showed the effect of –Cl positions in chlorophenols (CPs) degradation where CPs with a *para*- Cl atom, such as 2,4-DCP, were more easily removed because of the inhibitory effect of chlorine atoms at *meta*- position [63]. J. Araña et al. have also found that the *meta*- position was the less favored in the degradation of aminophenols [62]. As for nitrophenolic compounds the behavior was less sensitive to this parameter, due to a different electronic character, which caused a lower effect of the number of substituents and their positions on the initial photocatalytic degradation rate. Despite this, as the content of nitro groups increases the reaction rate decreases.

4. CONCLUSIONS

The efficiency of 4-CP and 4-NP photocatalytic degradation depends on initial concentration and presents different limits for complete removal, being 50 and 25 $mg \cdot L^{-1}$ respectively, in the studied experimental system. The photocatalytic degradation carries out with the formation of chloride and nitrogen inorganic ions in the reaction media that fulfills the Cl and N mass balances. The initial TOC photocatalytic degradation rate was not remarkably altered by the increase of pollutant concentration, although NPs are more initial concentration-sensitive.

The ecotoxicity of 4-NP is considerably lower than 4-CP, but after photocatalytic degradation both effluents resulted harmless, associated to the relevant conversion of pollutant.

The higher number of substituents modifies differently the kinetics, while the initial rate of chloride and nitrate formation speeds up, the overall TOC photocatalytic degradation rate slows down, with barely any changes in nitrite and ammonium formation. The ecotoxicity is not directly related with the number of chloro- and nitro- groups in the phenolic compound but to the position.

The effect of substituents position is complex to predict, with attack positions reinforced by the presence of substituents acting in concert. TOC photocatalytic degradation rate could be correlated to the electronic nature of substituents employing the Hammett constant. Chlorophenols resulted highly more affected than nitrophenols.

ACKNOWLEDGEMENTS

This work has been supported by the Spanish Plan Nacional de I+D+i through the project CTM2015-64895-R. Alvaro Tolosana-Moranchel thanks to Ministerio de Educación, Cultura y Deporte for his FPU grant (FPU14/01605). The authors are also grateful to Evonik Company for TiO_2 sample.

REFERENCES

[1] R. Hakulinen, S. Woods, J. Ferguson, M. Benjamin. The role of facultative anaerobic micro-organisms in anaerobic biodegradation of chlorophenols. Water Sci. Technol.17 (1985) 289-302

[2] J. Tremp, P. Mattrel, S. Fingler, W. Giger. Phenols and nitrophenols as tropospheric pollutants: emissions from automobile exhausts and phase transfer in the atmosphere. Water Air Soil Pollut. 68 (1993) 113-123

[3] S. Zhao, H. Ma, M. Wang, C. Cao, J. Xiong, Y. Xu, S. Yao. Study on the mechanism of photo-degradation of p-nitrophenol exposed to 254nm UV light. J Hazard Mater 180 (2010) 86-90. http://dx.doi:10.1016/j.jhazmat.2010.03.076

[4] P.K. Arora, A. Srivastava, V.P. Singh. Bacterial degradation of nitrophenols and their derivatives. J. Hazard. Mater. 266 (2014) 42-59. http://dx.doi.org/10.1016/j.jhazmat.2013.12.011

[5] E.B. Estrada-Arriaga, J.A. Zepeda-Aviles, L. García-Sánchez. Chemical Engineering Journal 285 (2016) 508-516

[6] E. Ferrer-Polonio, J.A. Mendoza-Roca, A. Iborra-Clara, J.L. Alonso-Molina, L. Pastor-Alcañiz. Journal of Industrial and Engineering Chemistry 43 (2016) 44-52

[7] R. Belloli, E. Bolzacchini, L. Clerici, B. Rindone, G. Sesana, V. Librando. Environ. Eng. Sci. 23 (2006) 405-415

[8] USEPA, Environmental Protection Agency, Environmental Criteria, Assessment Office. Cicinnati, OH: US, 1985

[9] S. Malato, M.I. Maldonado, P. Fernández-Ibáñez, I. Oller, I. Polo, R. Sánchez-Moreno. Science in Semiconductor Processing 42 (2016) 15-23

[10] Y. Yang, H. Li, F. Hou, J. Hu, X. Zhang, Y. Wang. Facile synthesis of ZnO/Ag nanocomposites with enhanced photocatalytic properties under visible light. Materials Letters 180 (2016) 97-100

[11] X. Zhang, Y. Wang, F. Hou, H. Li, Y. Yang, X. Zhang, Y. Yang, Y. Wang. Effects of Ag loading on structural and photocatalytic properties of flower-like ZnO microspheres. Applied Surface Science 391 (2017) 476-483

[12] N. Liu, W. Huang, M. Tang, C. Yin, B. Gao, Z. Li, L. Tang, J. Lei, L. Cuia, X. Zhang. In-situ fabrication of needle-shaped MIL-53(Fe) with 1T-MoS_2 and study on its enhanced photocatalytic mechanism of ibuprofen. Chem. Eng. J. 359 (2019) 254-264

[13] Y.J. Cui, J.H. Huang, X.Z. Fu, X.C. Wang. Metal-free photocatalytic degradation of 4-chlorophenol in water by mesoporous carbon nitride semiconductors. Catal. Sci. Technol. 2 (2012) 1396-1402

[14] A. Sharma, B.K. Lee. Integrated ternary nanocomposite of TiO_2/NiO/reduced graphene oxide as a visible light photocatalyst for efficient degradation of o-chlorophenol. Journal of Environmental Management 181 (2016) 563-573

[15] K. Bustos-Ramírez, C. E. Barrera-Díaz, M. De Icaza-Herrera, A. L. Martínez-Hernández, R. Natividad-Rangel, C. Velasco-Santos. 4-Chlorophenol removal from water using graphite and graphene oxides as photocatalysts. Journal of Environmental Health Science & Engineering (2015) 13-33. http://dx.doi.org/10.1186/s40201-015-0184-0.

[16] M. Faraldos, A. Bahamonde. Environmental applications of titania-graphene photocatalysts. Catalysis Today 285 (2017) 13-28

[17] X. Zhang, Y. Yang, W. Huang, Y. Yang, Y. Wang, C. He, N. Liu, M. Wu, L. Tang. g-C_3N_4/UiO-66 nanohybrids with enhanced photocatalytic activities for the oxidation of dye under visible light irradiation. Mater. Res. Bull. 99 (2018) 349-358

[18] Y. Gao, S. Li, Y. Li, L. Yao, H. Zhang. Accelerated photocatalytic degradation of organic pollutant over metal-organic framework MIL-53(Fe) under visible LED light mediated by persulfate. Appl. Catal. B. 202 (2017) 165-174

[19] W. Gernjak, M.I. Maldonado, S. Malato, J. Caceres, T. Krutzler, A. Glaser, R. Bauer. Solar Energy 77 (2004) 567-572

[20] U.M. Gaya, A.H. Abdullah. Journal of Photochemistry and Photobiology C: Photochemistry Reviews 9 (2008) 1-12

[21] M.G. Alalm, A. Tawfik, S. Ookawara. Journal of Water Process Engineering 8 (2015) 55-63

[22] R. Žabar, M. Sarakha, A.T. Lebedev, O.V. Polyakova, P. Trebše. Chemosphere 144 (2016) 615-620

[23] C. Berberidou, V. Kitsiou, E. Kazala, D.A. Lambropoulou, A. Kouras, C.I. Kosma, T.A. Albanis, I.Poulios. Applied Catalysis B: Environmental 200 (2017) 150-163

[24] F. Méndez-Arriaga, S. Esplugas, J. Giménez. Water Research 42 (2008) 585-594

[25] L.A. Ioannou, E. Hapeshi, M.I. Vasquez, D. Mantzavinos, D. Fatta-Kassinos. Solar Energy 85 (2011) 1915-1926

[26] L. Haroune, M. Salaun, A. Ménard, C.Y. Legault, J-P. Bell. Science of the Total Environment 475 (2014) 16-22

[27] Y. He, N.B. Sutton, H.H.H. Rijnaarts, A.A.M. Langenhoff. Applied Catalysis B: Environmental 182 (2016) 132-141

[28] J. A. Rengifo-Herrera, C. Pulgarin. Solar Energy 84 (2010) 37-43

[29] R. Fagan, D.E. McCormack, D.D. Dionysiou, S.C. Pillai. Materials Science in Semiconductor Processing 42 (2016) 2-14

[30] J. Lea, A.A. Adesina. J. Chem. Technol. Biotechnol. 76 (2001) 803-810

[31] M. Pera-Titus, V. Garcia-Molina, M.A. Banos, J. Gimenez, S. Esplugas. Appl. Catal. B: Environ. 47 (2004) 219-256

[32] E. Pino, M.V. Encinas. Journal of Photochemistry and Photobiology A: Chemistry 242 (2012) 20-27

[33] J. Chen, H. Zhang, P. Liu, Y. Li, X. Liu, G. Li, P.K. Wong, T. An, H. Zhao. Applied Catalysis B: Environmental 168-169 (2015) 266-273

[34] A. Shokri, K. Mahanpoor, D. Soodbar. Journal of Environmental Chemical Engineering 4 (2016) 585-598

[35] K. Zhang, Y. Liu, J. Deng, S. Xie, H. Lin, X. Zhao, J. Yang, Z. Han, H. Dai. Applied Catalysis B: Environmental 202 (2017) 569-579

[36] A. Tolosana-Moranchel, J.A. Anderson, J. A. Casas, M. Faraldos, A. Bahamonde. Journal of Environmental Chemical Engineering, 5(5) (2017) 4612-4620

[37] M. Ksibi, A. Zemzemi, R. Boukchina. Journal of Photochemistry and Photobiology A: Chemistry 159 (2003) 61-70

[38] M.H. Priya, G. Madras. Ind. Eng. Chem. Res. 45 (2006) 482-486

[39] T. Ohno, K. Sarukawa, K. Tokieda, M. Matsumura. Morphology of a TiO_2 Photocatalyst (Degussa, P-25) consisting of anatase and rutile crystalline phases. Journal of Catalysis 203 (2001) 82–86. http://dx.doi.org/10.1006/jcat.2001.3316

[40] B. Ohtani, O.O. Prieto-Mahaney, D. Li, R. Abe. What is Degussa (Evonik) P25? Crystalline composition analysis, reconstruction from isolated pure particles and photocatalytic activity test. Journal of Photochemistry and Photobiology A:Chemistry 216 (2010) 179-182

[41] J. Ryu, W. Choi. Substrate-Specific Photocatalytic Activities of TiO2 and Multiactivity Test for Water Treatment Application. Environ. Sci. Technol. 2008, 42, 294–300. http://dx.doi.org/10.1021/es071470x

[42] A. Tolosana-Moranchel, A. Montejano, J.A. Casas, A. Bahamonde. Elucidation of the photocatalytic-mechanism of phenolic compounds." Journal of Environmental Chemical Engineering 6(5) (2018) 5712-5719

[43] A. Tolosana-Moranchel, J. Carbajo, M. Faraldos, A. Bahamonde. Solar-assisted photodegradation of isoproturon over easily recoverable titania catalysts. Environ. Sci. Pollut. Res. 24 (2017) 7821-7828

[44] P. Garcia-Muñoz, J. Carbajo, M. Faraldos, A. Bahamonde. J. Photochem.Photobiol. A: Chem. 287 (2014) 8-18

[45] ISO 11348-3:1998, Water quality - Determination of the inhibitory effect of water samples on the light emission of Vibrio fischeri (Luminescent bacteria test) - Part 3: Method using freeze-dried bacteria

[46] Y.B. Wang, C.S. Hong. Water Res. 33 (1999) 2031–2036

[47] N. San, A. Hatipoğlu, G. Koçtürk, Z. Çınar, Journal of Photochemistry and Photobiology A: Chemistry 146(3) (2002) 189-97

[48] T. Egerton, P. Christensen, R Harrison, J. Wang. Journal of Applied Electrochemistry. 35(7) (2005) 799-813

[49] R. Vargas, O. Núñez. Journal of Molecular Catalysis A: Chemical. 300(1-2) (2009) 65-71

[50] E. Diaz, M. Cebrian, A. Bahamonde, M.Faraldos, A.F. Mohedano, J.A. Casas, J.J. Rodriguez. Catalysis Today 266 (2016) 168-174

[51] A. Di Paola, V. Augugliaro, L. Palmisano, G. Pantaleo, E. Savinov. J. Photochem. Photobiol. A-Chem. 155(1-3) (2003) 207-214

[52] W. Zhang, X. Xiao, T. An , Z. Song, J. Fu, G. Sheng. Journal of Chemical Technology & Biotechnology. 78(7) (2003) 788-94

[53] A. Hernández-Gordillo, A.G. Romero, F. Tzompantzi, R. Gómez. Applied Catalysis B: Environmental 144 (2014) 507-513

[54] H.Y. Gao, L. Mao, B. Shao, C.H. Huang, B.Z. Zhu. Scientific Reports 6 (2016) 33159

[55] T. Urbański. The chemistry of the nitro and nitroso groups. Ed. HENRY FEUER. Purdue University, Lafayette, Indiana. Part 2. Interscience Publishers (John Wiley & Sons) 1970. New York-London-Sydney-Toronto

[56] W.Z. Tang. Waste Management 15 (1995) 615-622

[57] K. Tanaka, W. Luesaiwong, T. Hisanaga. Journal of Molecular Catalysis A, Chemical 122(1) (1997) 67-74

[58] M. Muñoz, Desarrollo y combinación de procesos catalíticos de oxidación e hidrodecloración para el tratamiento de aguas contaminadas con clorofenoles. PhD Thesis. UAM. Madrid 2012

[59] I.M.S. Pillai, A.K. Gupta. Journal of Electroanalytical Chemistry. 756 (2015) 108-17

[60] C.P. Huang, C. Dong, Z. Tang. Waste Management 13 (1993) 361-377

[61] S. Parra, J. Olivero, L. Pacheco, C. Pulgarin. Applied Catalysis B: Environmental 43 (2003) 293-301

[62] J. Araña, J.M. Doña-Rodríguez, D. Portillo-Carrizo, C. Fernández-Rodríguez, J. Pérez-Peña, O. González Díaz, J.A. Navío, M. Macías. Applied Catalysis B: Environmental 100 (2010) 346-354

[63] J.-C. D'Oliveira, C. Minero, E. Pelizzetti, P. Pichat. Journal of Photochemistry and Photobiology A: Chemistry 72 (1993) 261-267.

[64] J.A. Dean, Lange's Handbook of Chemistry, 15 th ed., McGraw-Hill, New York, 1998.

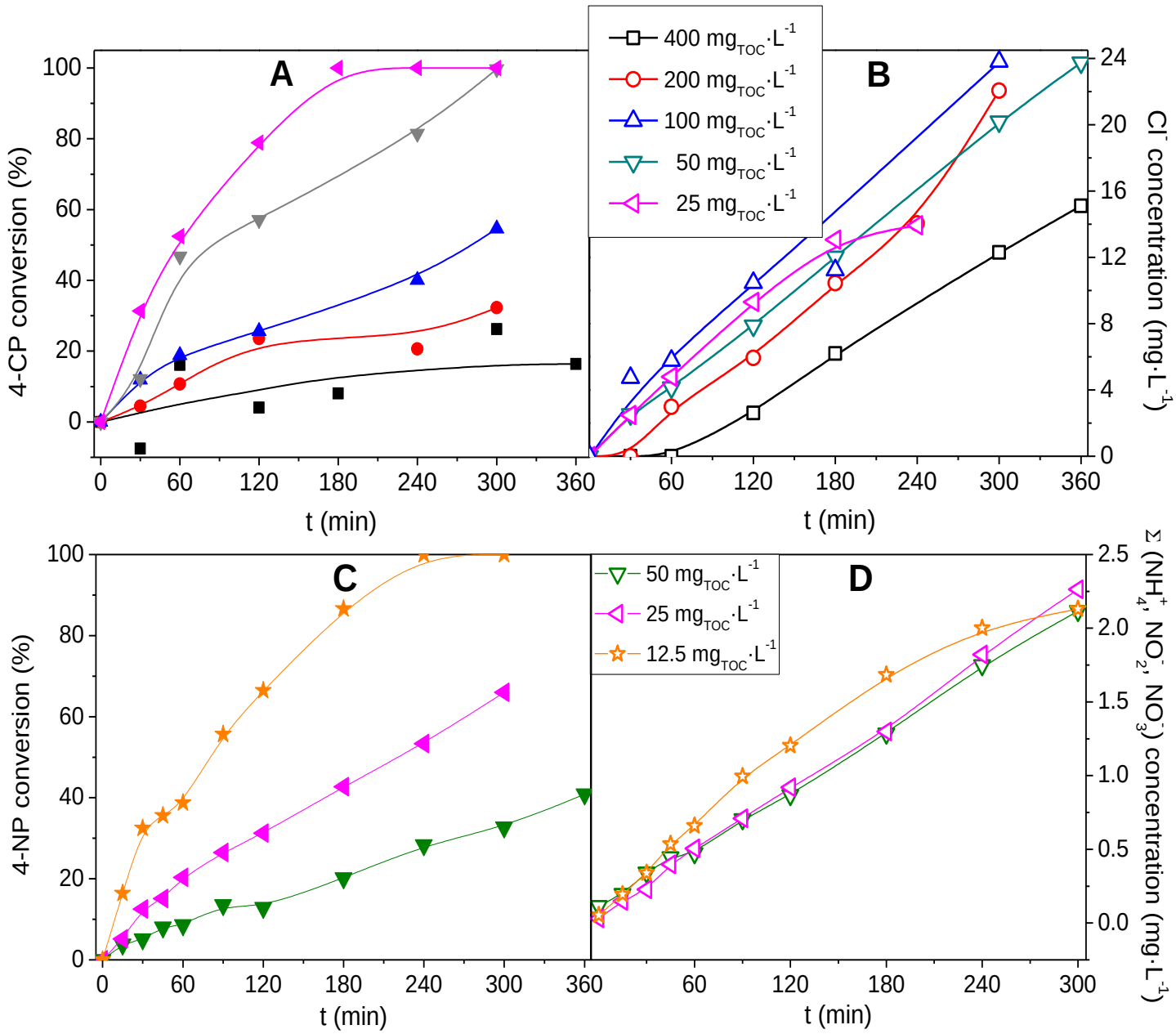

Figure 1. A) Evolution of 4-CP conversion, corresponding to 400-25 $mg_{TOC}·L^{-1}$ initial concentration. B) Formation of chloride. C) Evolution of 4-NP conversion, corresponding to 50-12.5 $mg_{TOC}·L^{-1}$ initial concentration. D) Formation of inorganic nitrogen ions (ammonium, nitrite and nitrate), calculated as N_{Total}.

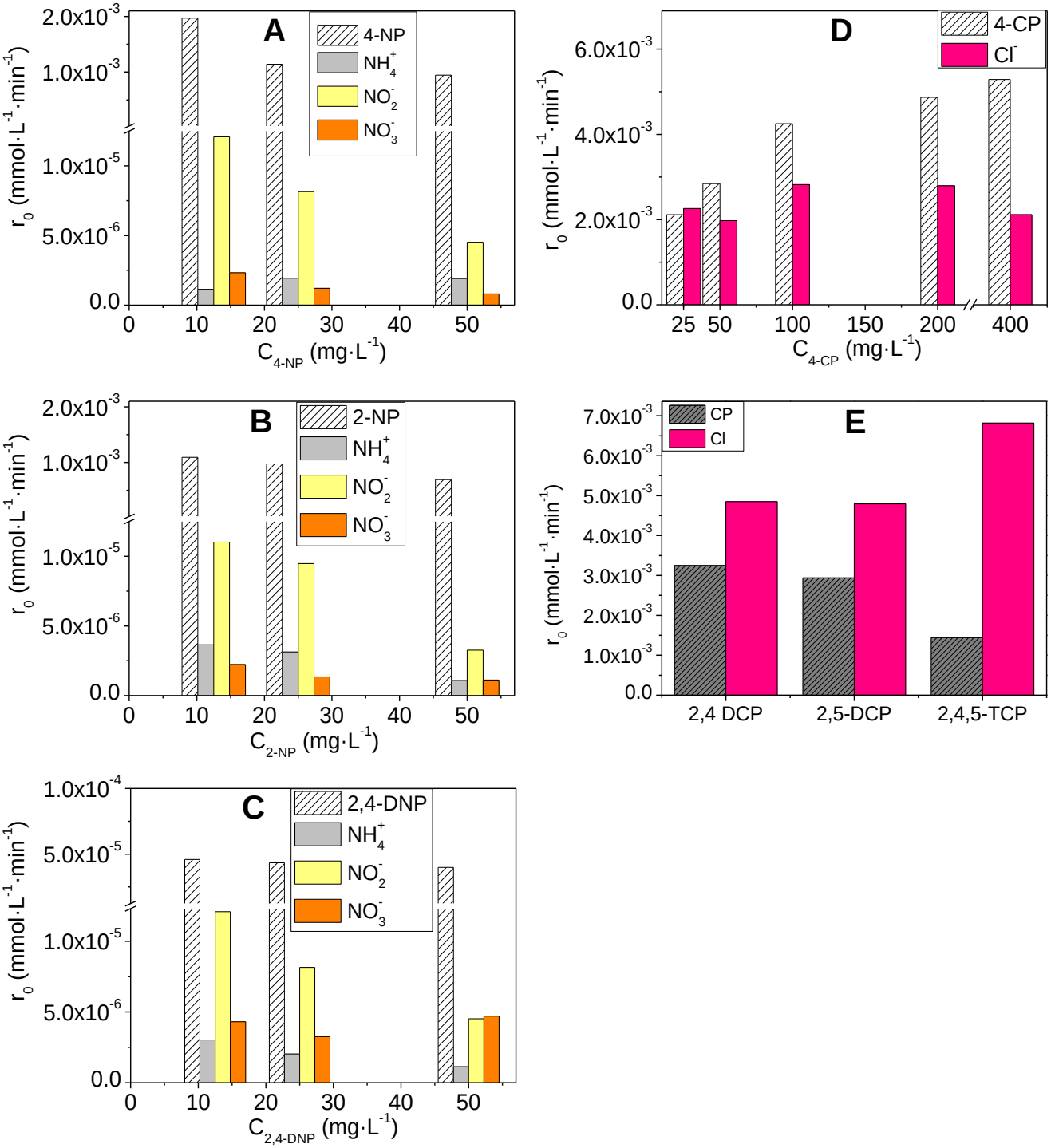

Figure 2. Initial rates of photocatalytic degradation and formation of ammonium, nitrite and nitrate ions for: 4-NP (A), 2-NP (B) and 2,4-DNP (C), at 12.5-50 $mg_{TOC}·L^{-1}$. Initial rates of photocatalytic degradation and formation of chloride ion for: 4-CP at 25-400 $mg_{TOC}·L^{-1}$ (D), and 2,4-DCP; 2,5-DCP and 2,4,5-TCP (E), at 50 $mg_{TOC}·L^{-1}$ concentration.

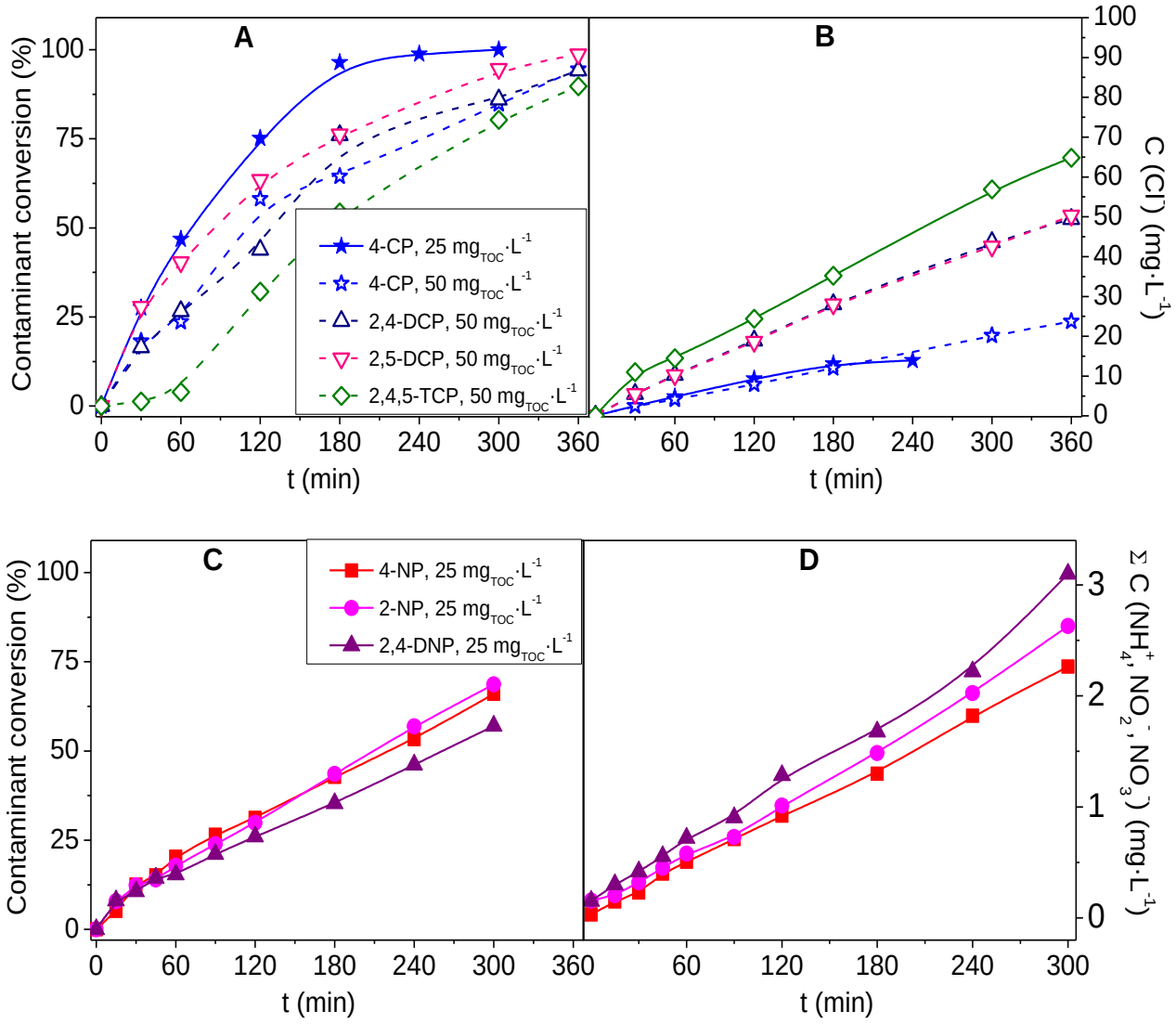

Figure 3. A) Evolution of CPs conversion at 50 $mg_{TOC}·L^{-1}$ initial concentration (4-CP evolution has been represented at 25 and 50 $mg_{TOC}·L^{-1}$ for comparative purpose), B) Formation of chloride; during CPs photocatalytic degradation reaction; C) Evolution of NPs conversion at 25 $mg_{TOC}·L^{-1}$ initial concentration, and D) Formation of inorganic nitrogen ions; during NPs photocatalytic degradation reaction.

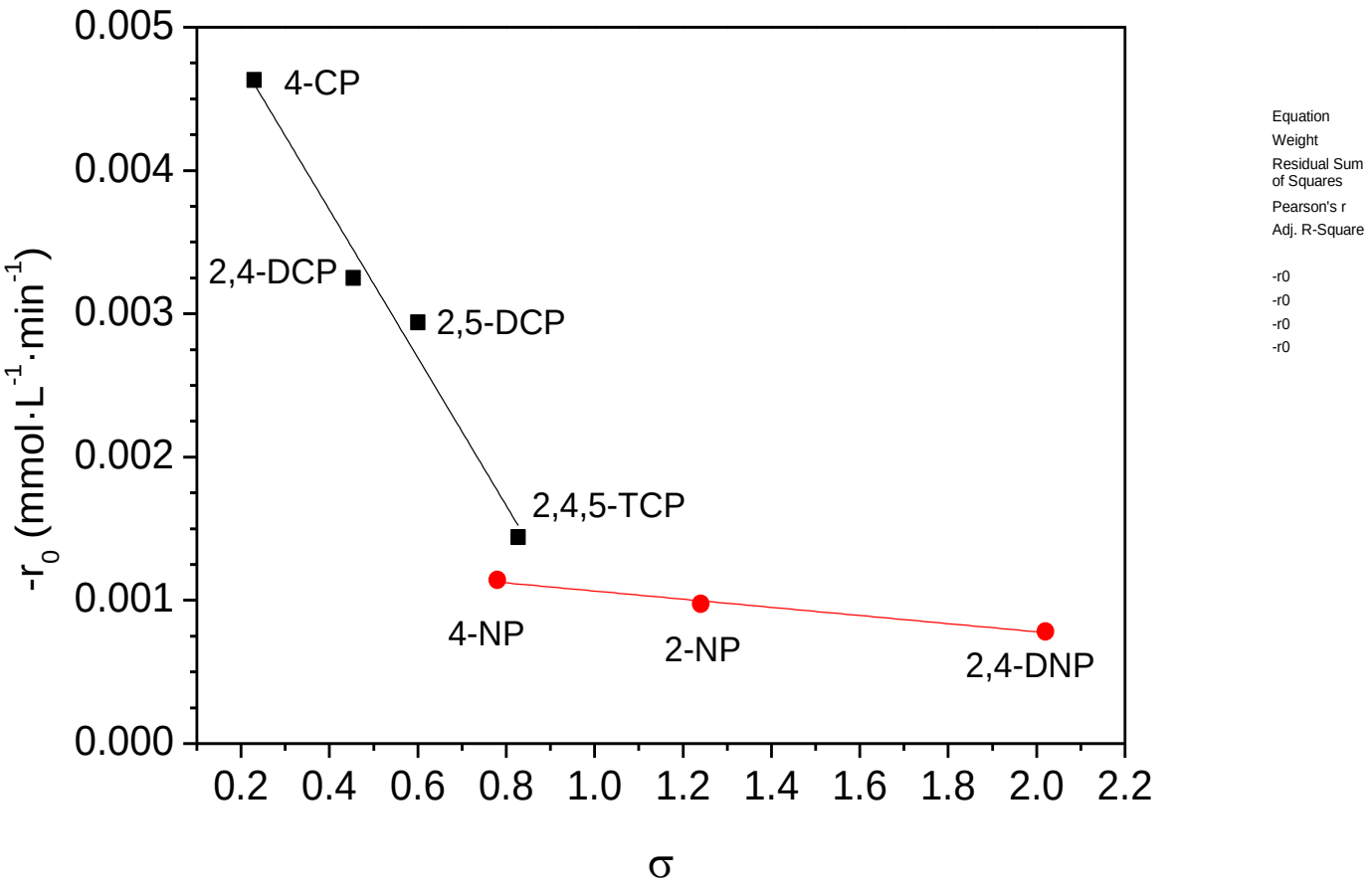

Figure 4. Correlation between Hammett constants and the initial photocatalytic degradation rate of CPs and NPs contaminants, at initial concentration of 50 $mg_{TOC}·L^{-1}$ and 25 $mg_{TOC}·L^{-1}$, respectively.

Table 1. Conversion of TOC, contaminants and inorganic ions, concentration of photocatalytic degradation inorganic products: Cl^-, NO_2^-, NO_3^- and NH_4^+, at 300 minutes of irradiation time, and kinetic parameters; for 4-CP and 4-NP.

4-Chlorophenol						4-Nitrophenol			
$[TOC]_0$[1] ($mg \cdot L^{-1}$)	**400**	**200**	**100**	**50**	**25**	**$[TOC]_0$**[1] ($mg \cdot L^{-1}$)	**50**	**25**	**12.5**
X_{TOC} (%)	7	15	30	73	99	**X_{TOC}** (%)	22	57	95
$X_{4\text{-}CP}$ (%)	13	32	53	85	99	**$X_{4\text{-}NP}$** (%)	34	66	99
$[Cl]_{0\ in\ 4\text{-}CP}$ ($mg \cdot L^{-1}$)	184	105	52	27	13	**$[N]_{0\ in\ 4\text{-}NP}$** ($mg \cdot L^{-1}$)	9	4.8	2.5
$[Cl^-]_{f\ in\ reaction\ media}$ ($mg \cdot L^{-1}$)	12	22	24	21	13	**$[\Sigma NH_4^+, NO_2^-, NO_3^-]_{f\ in\ reaction\ media}$**[2] ($mg \cdot L^{-1}$)	2.1	2.5	2.3
$[Cl^-]_{f\ in\ Cl\text{-}intermediates}$[3] ($mg \cdot L^{-1}$)	13	20	1	1	0	**$[\Sigma N]_{f\ in\ N\text{-}intermediates}$**[4] ($mg \cdot L^{-1}$)	0	0.3	0.2
X_{Cl} (%)	7	21	46	76	99	**X_N** (%)	24	52	89
$(-r_{TOC})_0$ ($mg \cdot L^{-1} \cdot min^{-1}$)	0.13	0.13	0.12	0.11	0.13	**$(-r_{TOC})_0$** ($mg \cdot L^{-1} \cdot min^{-1}$)	0.015	0.047	0.063

[1] Theoretical values; [2] Calculated as N_{total} ; [3] 4-Chlorocathecol, expressed as Cl^-; [4] 4-Aminophenol, expressed as N

Table 2. Conversions at 300 minutes of irradiation time and TOC initial rates for the studied chloro- and nitrophenols.

	Chlorophenols ($25\ mg_{TOC}\cdot L^{-1}$)	**Chlorophenols ($50\ mg_{TOC}\cdot L^{-1}$)**				**Nitrophenols ($25\ mg_{TOC}\cdot L^{-1}$)**		
	4-CP	**4-CP**	**2,4-DCP**	**2,5-DCP**	**2,4,5-TCP**	**4-NP**	**2-NP**	**2,4-DNP**
$X_{CP\ /\ NP}$ (%)	100	96	85	87	80	66	69	57
X_{TOC} (%)	100	73	69	69	58	57	61	35
$(-r_{TOC})_0$ ($mg\cdot L^{-1}\cdot min^{-1}$)	0.13	0.10	0.12	0.10	0.13	0.047	0.057	0.028

Table 3. Reduction of ecotoxicity and TOC on photocatalytic degradation during 360 minutes for CPs and 300 minutes for NPs.

	Chlorophenols (50 $mg_{TOC} \cdot L^{-1}$)				Nitrophenols (12.5 $mg_{TOC} \cdot L^{-1}$)		
	4-CP	**2,4-DCP**	**2,5-DCP**	**2,4,5-TCP**	**4-NP**	**2-NP**	**2,4-DNP**
EC50 ($mg \cdot L^{-1}$)	1.8	3.5	8.9	1.5	7.5	36.8	37.4
Initial ecotoxicity (TU)	52	33	14	98	3.8	0.85	0.75
Final ecotoxicity (TU)	11	14	2	5	0.1	0.1	0.1
ΔTU[1] (%)	79	57	87	95	100	100	100
X_{TOC}[2] (%)	88	83	83	71	95	92	88

[1] ΔTU: reduction of ecotoxicity by Microtox test. [2] The irradiation time was longer for CPs to assure enough mineralization degree and absence of toxic intermediates.

Supplementary Material

Click here to download Supplementary Material: Figures SI_F.docx